Solidification of a binary mixture saturating an inclined bed of packed spheres

C.-H. Yang, S. K. Rastogi and D. Poulikakos
Mechanical Engineering Department, University of Illinois at Chicago, Chicago, IL, USA

In this paper, an experimental study is reported for the problem of freezing of a binary mixture (water and NH_4Cl) saturating an inclined bed of spheres. Two different beds consisting of spheres with markedly different thermal conductivities (glass and steel) were studied. The effect of the inclination angle of the bed with respect to the gravity vector, on the temperature field in the bed and on the interface shape between the solid and the mixed phase regions, was determined. Engineering correlations are reported for the dependence of the volume of the completely frozen region on time for both the steel-bead bed and the glass-bead bed for representative initial concentrations.

Keywords: binary alloys; phase change; porous materials

Introduction

The process of freezing of mixtures and alloys saturating a solid matrix occurs in a variety of applications. Examples include the freezing of soils and rocks in geology, freezing of food products in the food processing industry, manufacturing of composites in the materials industry, and energy storage. Furthermore, in bioengineering applications of cryosurgery and cryopreservation, control over the solidification pattern in biological tissues and cells of organs is essential. Unlike the solidification of a pure substance, the phenomenon of freezing of mixtures and alloys is characterized by the simultaneous occurrence of heat flow, fluid flow, and species transport.

The solidification of mixtures and alloys in the absence of a porous matrix has been extensively studied in recent years (see, for example, Bennon and Incropera 1987a, 1987b; Cao and Poulikakos 1990; Chellaiah and Viskanta 1987; Chen and Chen 1991; Christenson and Incropera 1989; Thompson and Szekeley 1988). A review of the subject (Huppert 1990) is also available. It is now well recognized that the transport processes occurring due to the existence of the thermal, and possibly the solutal, gradients have a strong effect on the progress of the freezing process and on the morphology of the resulting solid. On the other hand, the studies on the freezing of multicomponent substances saturating a porous matrix are limited. Here, the phase-change process eventuates in the pores of the solid matrix, and it is such that three distinct regions exist simultaneously. In the first region, the pores of the solid matrix are filled by the frozen solid. The second region (often termed as the mushy zone or the mixed-phase region) is characterized by the existence of a complex composite of solid flakes or dendrites and liquid in the pores of the solid matrix. In this region, the transport phenomena involve interaction among three different phases, namely, the solid constituting the matrix, the solid constituting the flakes or dendrites, and the liquid. Fluid motion is often possible in this region as a result of the existence of the thermal and the solutal gradients. The third region is simply the part of the porous matrix saturated with the fluid that has not solidified yet. The mushy zone separates the solid from the liquid region. Representative studies on the freezing of liquid-saturated porous media are reviewed next.

Even though the present study pertains to the solidification of a multicomponent mixture in a bed of packed spheres, some of the relevant work on solidification in a porous medium saturated with a pure substance will be discussed first. Gupta and Churchill (1971) studied the heat and moisture migration in wet sand during freezing. They reported that the water migrated to the freezing front and solidified, resulting in an increase in the water content of the frozen sand and a decrease in the water content of the unfrozen sand. Goldstein and Reid (1978) proposed an analytical solution using the methods of the complex variable theory for the problem of freezing of a water-saturated porous medium. Hashemi and Sliepevich (1973) conducted a numerical study using the finite-element method to model the freezing around a row of pipes embedded in a porous medium. A similar study was performed by Frivik and Comini (1982) to model the freezing and thawing of soil in the presence of seepage flow using the finite-element method. The predicted temperatures were compared successfully with experimental data from a laboratory model of a soil-freezing system. Sugawara et al. (1988) examined the effect of the maximum density of water on the freezing of a water-saturated horizontal porous layer. The agreement between theory and experiment was good. Weaver and Viskanta (1986) reported experimental and analytical studies on the freezing of a water-saturated porous medium enclosed in a cylindrical capsule and cooled from the outside for vertical as well as horizontal orientations. Chellaiah and Viskanta (1988) studied the freezing of saturated and superheated water in porous media enclosed in a rectangular cavity. To this end, they examined the effects of the glass-bead size, the imposed temperature difference, and the liquid superheat. For freezing of saturated water, good

Address reprint requests to Professor Poulikakos at the Mechanical Engineering Department, University of Illinois at Chicago, P.O. Box 4348, Chicago, IL 60680, USA.

Received 23 June 1992; accepted 25 November 1992

agreement was reported between the experimental temperature distribution and the temperature distribution predicted by a one-dimensional (1-D) heat conduction model. In a later study (Chellaiah and Viskanta 1989), the same authors developed a numerical model based on the volumetric averaging of the macroscopic transport equations, with phase change assumed to take place volumetrically over a small temperature range. The results of the numerical model were compared successfully to the experimental data.

With regard to the solidification in a porous matrix saturated with a multicomponent mixture, to the best of the authors' knowledge the available (published) research is very limited. We cite two such studies, the theoretical work of Kececioglu and Rubinsky (1989) and the experimental study of Cao and Poulikakos (1991). Kececioglu and Rubinsky (1989) developed a continuum model for the propagation of discrete phase-change fronts in porous media in the presence of coupled heat flow, fluid flow, and species transport processes. In addition, they specialized the theory to the problem of melting or freezing interfaces in a salt-water saturated porous medium. Cao and Poulikakos (1991) reported the findings of an experimental study on the solidification of a water–NH_4Cl mixture saturating a packed bed of spheres. The system was cooled from its top surface. The effect of heating the bottom surface of the system simultaneously with cooling the top surface was also examined. Additionally, a simple analytical model that neglected convection was reported.

The present paper reports the main procedures and results of an experimental investigation of the problem of transient solidification of a binary mixture (NH_4Cl–H_2O) saturating a packed bed of beads enclosed in an inclined rectangular cavity. Note that the choice of this mixture was based on the fact that it is easy to work with, it solidifies at relatively high temperatures, and it possesses an equilibrium phase diagram qualitatively (and quantitatively) similar to mixtures of a host of other salts (such as NaCl) existing in considerable quantities in soil and in food processing. The present being a basic study, it will provide results on the trends in the freezing of salt mixtures in packed beds of beads for several salts with similar equilibrium phase diagrams, not only for mixtures of NH_4Cl. This study is novel because it focuses on the effect of the orientation of the cooling surface with respect to the gravity vector on the solidification phenomenon of interest. The entire range of the orientation angle (0°–180°) is examined for two types of beds of beads with markedly different thermal conductivities (glass and steel, respectively) and for two different initial concentrations of the solute in the mixture. The reported results include the effect of the orientation angle on the evolving temperature field and on the shape of the solid/mush interface. Additionally, the dependence of the volume of the frozen region on the inclination angle, on the initial concentration, and on time is summarized in engineering correlations for both the bed of glass beads and the bed of steel beads.

Experimental apparatus and procedure

The freezing experiments were conducted in a rectangular test cell. A schematic of this cell is shown in Figure 1. The dimensions of the enclosed liquid-saturated porous medium

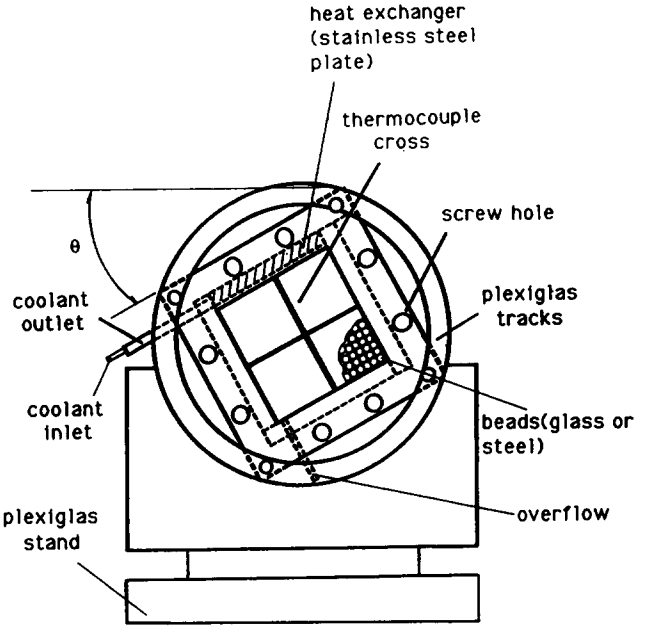

Figure 1 Schematic of the test section

Notation

A	Constant, Equation 2 and Table 1
c	Specific heat
C	Concentration of solute, wt-percent
d	Bead diameter
Fo	Fourier number, Equation 1
L	Latent heat of fusion, Equation 1
Ste	Stefan number, Equation 1
t	Time, min
T	Temperature, °C
V	Frozen solid volume, m^3
V_T	Total volume of the cavity, m^3
V^*	Dimensionless frozen solid volume, V/V_T

Greek symbols

α	Thermal diffusivity, m^2/s
β	Constant, Equation 2 and Table 1
ε	Constant, Equation 2 and Table 1
θ	Inclination angle
λ_1	Constant
λ_2	Constant
τ	Dimensionless time, Equation 1
ϕ	Porosity
ψ	Constant, Equation 2 and Table 1

Subscripts

eut	Eutectic
f	Fusion
i	Initial
ms	Volume-weighted in the solid region
s	Solid

measured 51 mm in length, 51 mm in height, and 57 mm in depth. The test section was mounted on two circular tracks as shown in Figure 1. These tracks facilitated the rotation of the cavity to effect the desired angle of inclination of the cold wall of the apparatus with respect to the gravity vector. Note that in doing so, all the three basic configurations (freezing along a "top" wall, a vertical "side" wall, and a "bottom" wall) were encountered. All the walls of the test apparatus were constructed out of Plexiglas of thickness 5.85 mm. Two Plexiglas sheets with a vacuum gap in between were used on the front and the back of the rectangular cavity so as to reduce the thermal interaction with the ambient, to eliminate the condensation of moisture, and to allow for the photographic and visual observations. The entire test cell was covered with 30-mm-thick styrofoam insulation, which helped practically to eliminate the heat exchange with ambient.

The cold wall of the apparatus was constructed out of stainless steel of thickness 6.85 mm. To achieve the desired cooling, this wall was machined to have a counterflow heat exchanger in the form of channels that allowed for the flow of the coolant. The flow channels in the plate were milled such that a uniform temperature of the cooling plate was achieved. To check the isothermality of the cooling plate, five copper and constantan thermocouples were installed on it. Indeed, the cooling plate was found to be isothermal within 0.2°C for all the experiments.

The temperature distribution in the liquid-saturated porous bed was monitored with a thermocouple grid placed at the centerplane of the cavity perpendicular to the cold wall (Figure 1). The grid was cut out of a thin Plexiglas sheet (1 mm in thickness) in the form of a cross that did not affect the porosity of the bed. The grid consisted of a total of 20 30-gauge copper and constantan thermocouples with 10 equidistant thermocouples in each direction (perpendicular and parallel to the cold wall; see Figure 1). The thermocouples were mounted through small holes drilled in the Plexiglas cross and were glued with epoxy. The thermocouple wires exited the enclosure through two small holes in the side walls of the enclosure that were sealed afterwards. These holes were connected to plastic tubes and also accommodated the volume expansion of the mixture upon freezing.

Spherical soda-lime glass beads and stainless steel beads of an average diameter of 5 mm (± 0.1 mm) created the porous matrix in the two sets of the experiments. Hence, the porosity (equal to 0.37) and the permeability were the same in the two systems. At this point it is worth addressing the issue of flow channeling resulting from porosity non-homogeneity near a solid wall bounding a packed bed (Chandrasekara and Vortmeyer 1979; Benenati and Brosilow 1962). The porosity variation with distance (y) away from a solid wall is given by Benenati and Brosilow (1962) as $\phi/\phi_\infty = 1 + \lambda_1 \exp(-\lambda_2 y/d)$ where ϕ is the porosity, d is the bead diameter, and λ_1, λ_2 are empirical constants depending on the bead size. The subscript ∞ denotes the region far away from and unaffected by the wall. For 5-mm-diameter beads, $\lambda_1 = 0.43$ and $\lambda_2 = 3$ (Benenati and Brosilow, 1962). Hence, utilizing the above equation for $y/d = 1$ (a distance of one bead diameter away from the wall) we obtain that $\phi/\phi_\infty = 1.021$. This result implies that the porosity has attained the value of the region far away from the wall, for all practical purposes. Clearly then, in the experiments of the present study, the porous bed is homogeneous at distances greater than one bead diameter away from the walls. Note further that since the height of the enclosure is 51 mm, the bead diameter is 5 mm and since the beads are well packed (not placed one on top of the other to form a column), at least 15 beads fit from top to bottom in the enclosure. Therefore, the results of the present study do model freezing in a homogeneous porous bed bounded by solid walls. A binary NH_4Cl–H_2O solution at room temperature was used as the saturating fluid of the porous medium. Two initial solute concentrations (of 5 wt-percent and 25 wt-percent) were studied. For each concentration, the experiments were performed by rotating the cavity from $\theta = 0°$ to 180° at intervals of 30°.

The procedure for obtaining the data was as follows. To begin an experiment, first the enclosure was packed completely with either the glass beads or the stainless steel beads, with the thermocouple grid kept in the centerplane perpendicular to the cold surface. Next, the enclosure was filled with a NH_4Cl–H_2O solution at room temperature (22°C) and of the desired initial uniform composition. Care was exercised to avoid air bubbles. The test section was then positioned at the desired angle with respect to the gravity vector. To effect the solidification process, the coolant in the refrigerator, which was precooled and kept at −25°C in all experiments, was suddenly circulated through the heat exchanger machined into the stainless steel wall of the apparatus. The imposed cooling resulted in a buoyancy-induced flow thereafter eventuating the solidification of the mixture. As solidification progressed, the temperature data were recorded using a data-acquisition system. The data-acquisition system consisted of a Hewlett-Packard 150 Touchscreen II PC, two Hewlett-Packard 3421A data-acquisition control units, a printer, and a Hewlett-Packard data-acquisition software package. Temperature measurements were recorded at one-minute time intervals. The accuracy of the temperature measurements was estimated to be within 3 percent and was dictated by the accuracy of the software that converted the voltage measurements to temperature.

The solid/mush interface was traced from photographs taken at several time intervals. The frozen solid volume was estimated by tracing the solid/mush interface at different times and, next, by measuring the area of the frozen layer by a digital planimeter. Note that our observations indicated that the solid/mush interface was essentially two-dimensional (2-D). For each solid/mush interface location, the area of the frozen layer was measured three times. The reported data points are based on the arithmetic mean of the three readings. A Nikon FE 35-mm camera with T-max ASA 400 black and white film was used to take the photographs used to trace the solid/mush interface. The tracing of the mush/liquid interface was not possible using the photographs, since it could not be precisely distinguished. Qualitative flow visualization in some experiments was accomplished by adding potassium permanganate crystals to the liquid and observing the traces of the resulting colored streaks. No velocities were measured.

Results and discussion

The main results of this study report the effect of the initial concentration of the binary mixture (NH_4Cl–H_2O) and of the inclination angle of the cooling surface with respect to the gravity vector on the transient freezing phenomenon of interest. For both the glass-bead bed and the steel-bead bed, experiments with the initial salt concentration of 5 wt-percent and 25 wt-percent were conducted. Relevant to this discussion is the equilibrium phase diagram of a water and NH_4Cl mixture (Stephen and Stephen 1963). The initial concentration of 5 wt-percent is located to the left of the eutectic point (Figure 2)

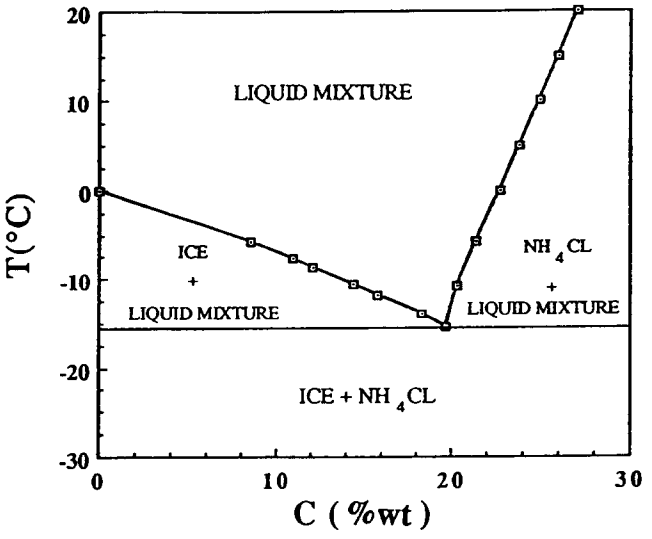

Figure 2 The equilibrium phase diagram for a water–NH_4Cl eutectic binary mixture

and is termed as hypoeutectic. For hypoeutectic concentrations, the freezing is characterized by a two-phase mushy region in which the dendrites are composed of ice. A water-lean fluid is rejected in the liquid phase at the mush/liquid interface. In the case of the initial concentration of 25 wt-percent (termed as hypereutectic and located to the right of the eutectic point; see Figure 2), solidification is characterized by rejection of water-rich interdendritic fluid. The dendrites in the mushy zone consist of NH_4Cl crystals. Note that the equilibrium freezing points of all solutions can be found from Figure 2.

The discussion of the results starts with the effect of the initial salt concentration and of the inclination angle on the transient temperature response of the cold wall. The temperature data are plotted versus time in Figure 3 for the initial concentration of 5 wt-percent. Figure 3a contains the data for the glass-bead bed, whereas Figure 3b shows the data for the steel-bead bed. In both cases, the wall temperature decreases rapidly at early times (approximately 10 minutes) and reaches a plateau at later times. Clearly, there is no appreciable indirect effect of the inclination angle on the cold wall temperature (the inclination angle is expected to affect the flow in the system). Moreover, for both beds, the cold wall temperature for the initial concentration of 25 wt-percent exhibited the same behavior (qualitatively) as for the initial concentration of 5 wt-percent shown in Figure 3. For the sake of brevity, the results of the cold wall temperature response for the initial concentration of 25 wt-percent are not presented here. In summary, regarding the temperature of the cold wall, as mentioned in the previous section a coolant maintained at a temperature of $-25°$ (for all experiments) was circulated through the heat exchanger machined in the cold wall at the initiation of the experiments. The resulting transient temperature of the cold wall is defined in Figures 3a and 3b.

The temperature field evolution is discussed next. Figures 4 and 5 illustrate the temperature distribution along the centerline of the porous bed perpendicular to the cold wall at five characteristic times for the glass beads and the steel beads, respectively. The reported temperature data in Figures 4 and 5 correspond to the initial salt concentration of 5 wt-percent. In both beds, the temperature increases as one moves away from the cold wall for all inclination angles and at all times. The top-to-bottom temperature difference (ΔT) is larger in the glass-bead matrix (Figures 4a–4f) than in the steel-bead matrix (Figures 5a–5f) at all times. For example, for identical experimental conditions in the steel-bead bed, the resulting ΔT was 20°C as opposed to $\Delta T = 30°C$ in the glass-bead bed at $t = 20$ minutes for $\theta = 0°$. Note that the thermal conductivity of the steel-bead matrix is much higher than that of the glass-bead matrix. Hence, the steel-bead matrix cannot sustain large temperature gradients.

The shape of the temperature distribution curves in Figures 4a–4f and 5a–5f verifies the existence of the convective flow during the solidification process, more so in the glass-bead bed. It should be noted here that for the initial

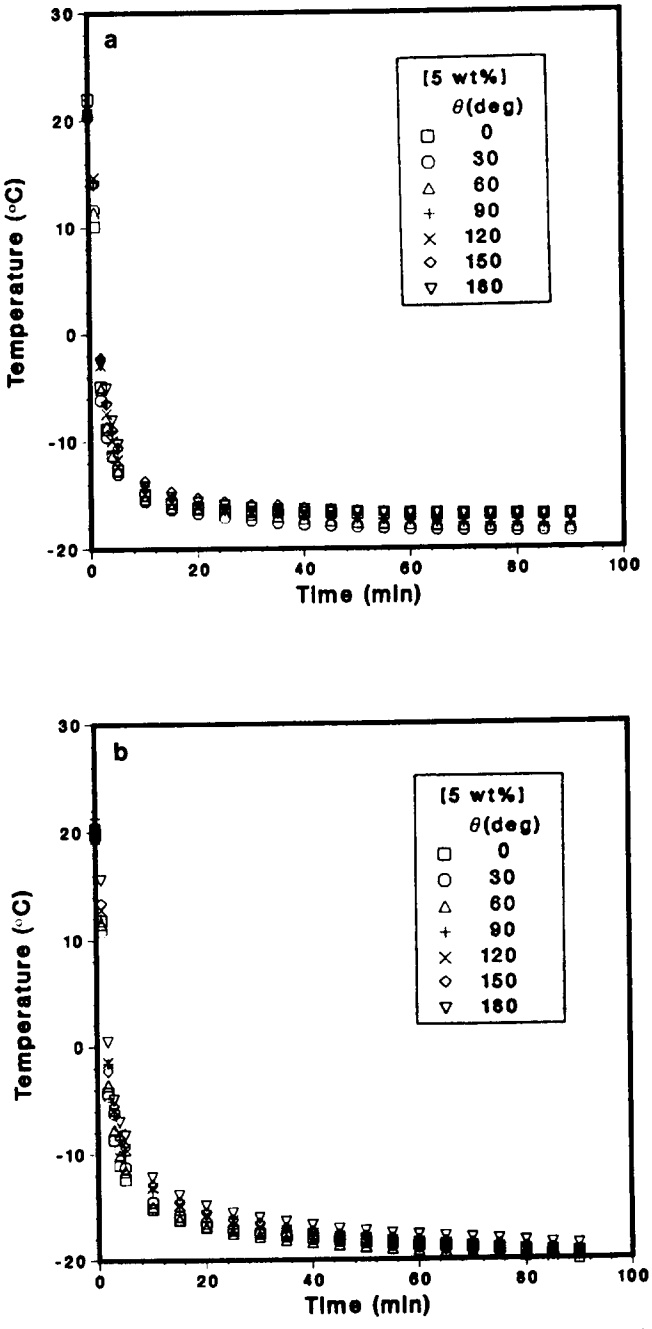

Figure 3 The temperature variation of the cold wall for the glass beads: (a) glass beads; (b) steel beads

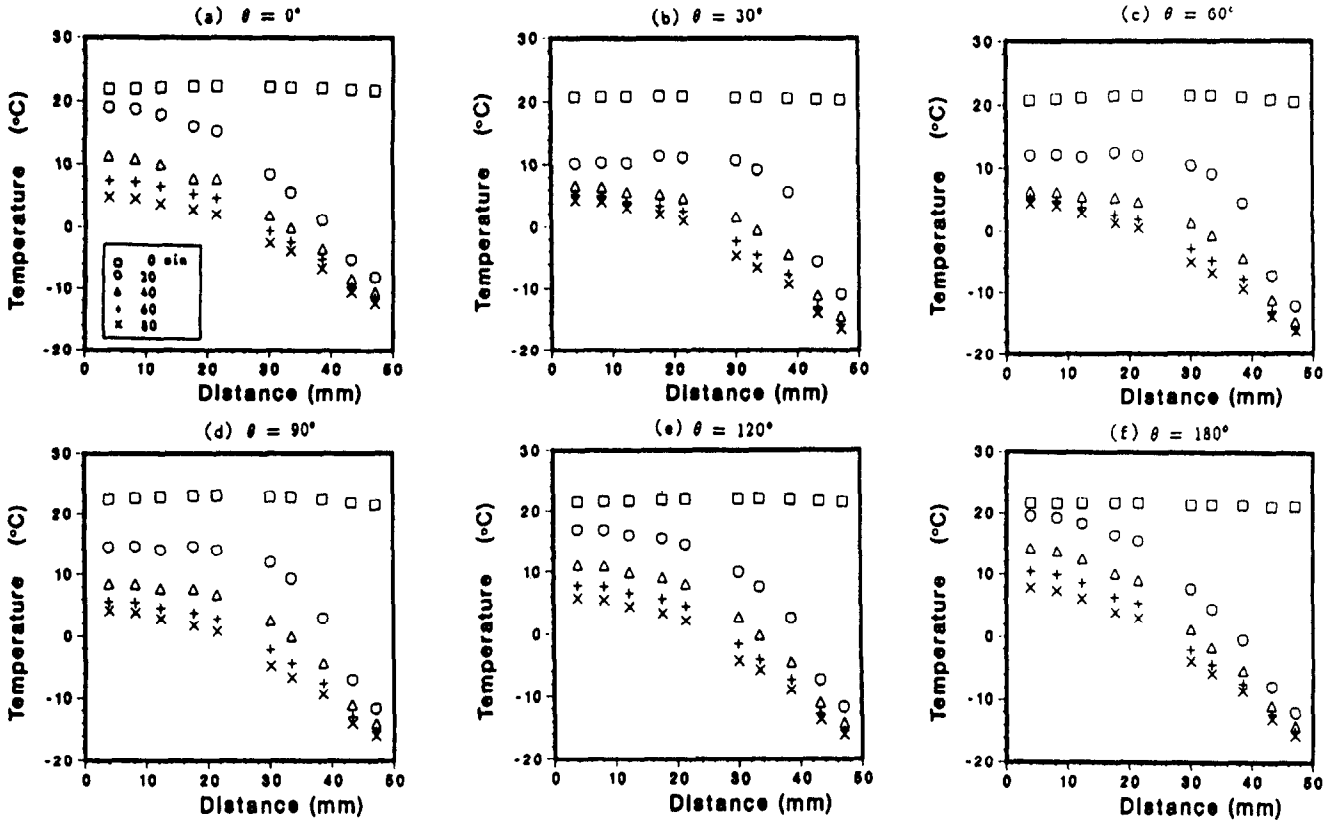

Figure 4 Temperature distribution at the centerline perpendicular to the cold wall in the glass-bead bed (C_i = 5 wt-percent). The distance is measured away from the bottom wall of the cavity, opposite to the cold wall

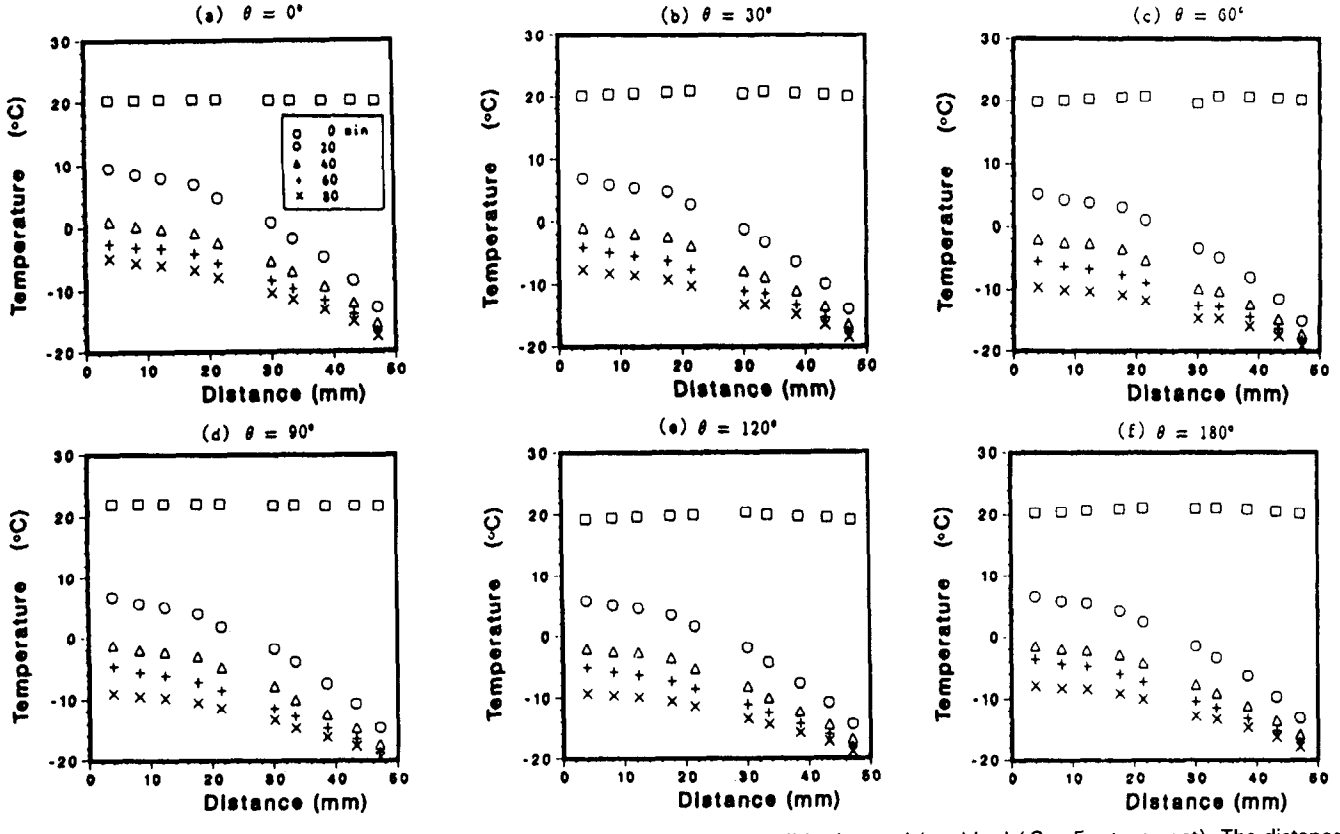

Figure 5 Temperature distribution at the centerline perpendicular to the cold wall in the steel-bead bed (C_i = 5 wt-percent). The distance is measured away from the bottom wall of the cavity opposite to the cold wall

concentration of 5 wt-percent, the thermal as well as the solutal gradients are expected to be aiding one another in creating the buoyancy-driven flow, since the freezing here is characterized by preferential incorporation of water crystallized ice at the phase-change interface. For $\theta = 180°$ (Figures 4f and 5f), even though both gradients (thermal and compositional) are stable since the cold plate is located on the underside, the convective nature of the temperature profile can still be observed. This is attributed to the density anomaly of water at 4°C. Detailed temperature distribution plots for the initial concentration of 25 wt-percent are omitted from here on due to space limitation; they are reported by Yang (1992).

Representative temperature distributions at the centerline of the enclosed porous space parallel to the cold wall are shown in Figures 6 and 7 for the glass-bead bed and the steel-bead bed, respectively. The data plotted in both these figures correspond to the initial concentration of 5 wt-percent. The temperature field at $t = 20$ and 40 minutes affirms the presence of the convection in the system for all inclination angles of interest. The effect of convective motion is more pronounced in the glass-bead bed (Figure 6) than in the steel-bead bed (Figure 7). As mentioned earlier, due to the high thermal conductivity of the steel-bead bed, large temperature gradients essential to the creation of natural convection flow cannot be sustained. This also explains the fact that the temperature distribution shows no noticeable dependence on the inclination angle for the steel beads.

The evolution of the freezing process is discussed next. Figures 8 and 9 show tracings of the solid/mush interface at characteristic times in the glass-bead bed and in the steel-bead bed and for the initial concentrations of 5 wt-percent and 25 wt-percent, respectively. A mushy zone of finite extent existed in all cases. However, the mush/liquid interface was not clearly distinct to be precisely traced. Nevertheless, the shape of this interface was not very different from the shape of the solid/mush interface. Furthermore, the region occupied by the solid and the mixed-phase zone grew with time (indicating the progress of the solidification phenomenon) for all the inclination angles of interest for both the hypoeutectic 5 wt-percent as well as the hypereutectic 25 wt-percent concentrations.

A comparison of Figures 8a and 8b reveals that the freezing occurs at a faster rate for the hypoeutectic initial concentration $C_i = 5$ wt-percent (Figure 8a) than for the hypereutectic initial concentration $C_i = 25$ wt-percent (Figure 8b). It is worth recalling that the solid in Figure 8a is ice, whereas the solid in Figure 8b is crystallized salt, which yields a more permeable mushy zone. As a result, convective fluid motion in this mushy zone retards the solidification.

The undulated shape of the solid/mush interface in Figures 8a and 8b is a direct result of the double-diffusive convection present in the system during the freezing process. For $C_i = 5$ wt-percent (Figure 8a), the shape of the interface implies the presence of bicellular convection in the bed for $\theta = 0°$. For

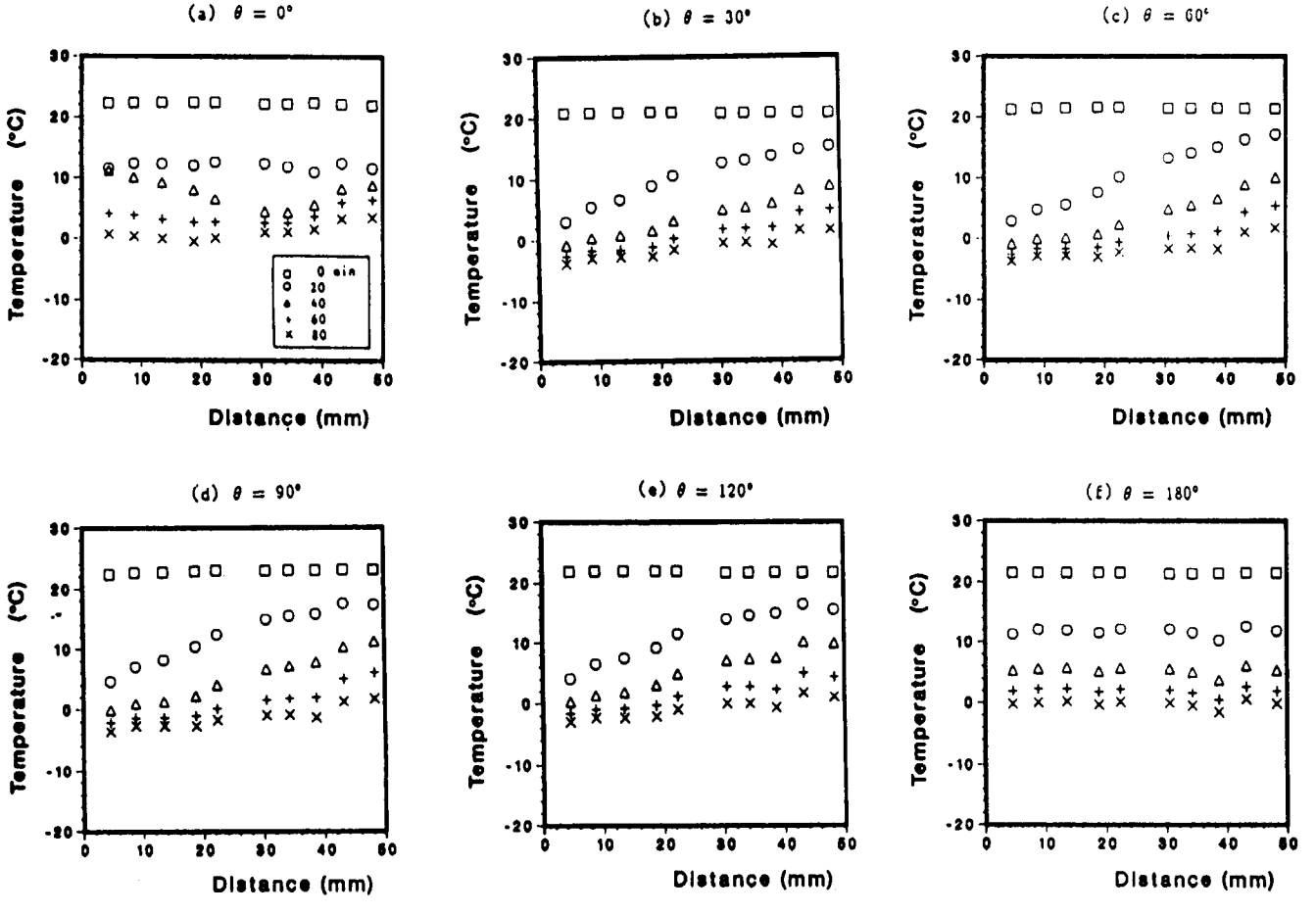

Figure 6 Temperature distribution at the centerline parallel to the cold wall in the glass-bead bed ($C_i = 5$ wt-percent). The distance is measured away from the left wall of the cavity

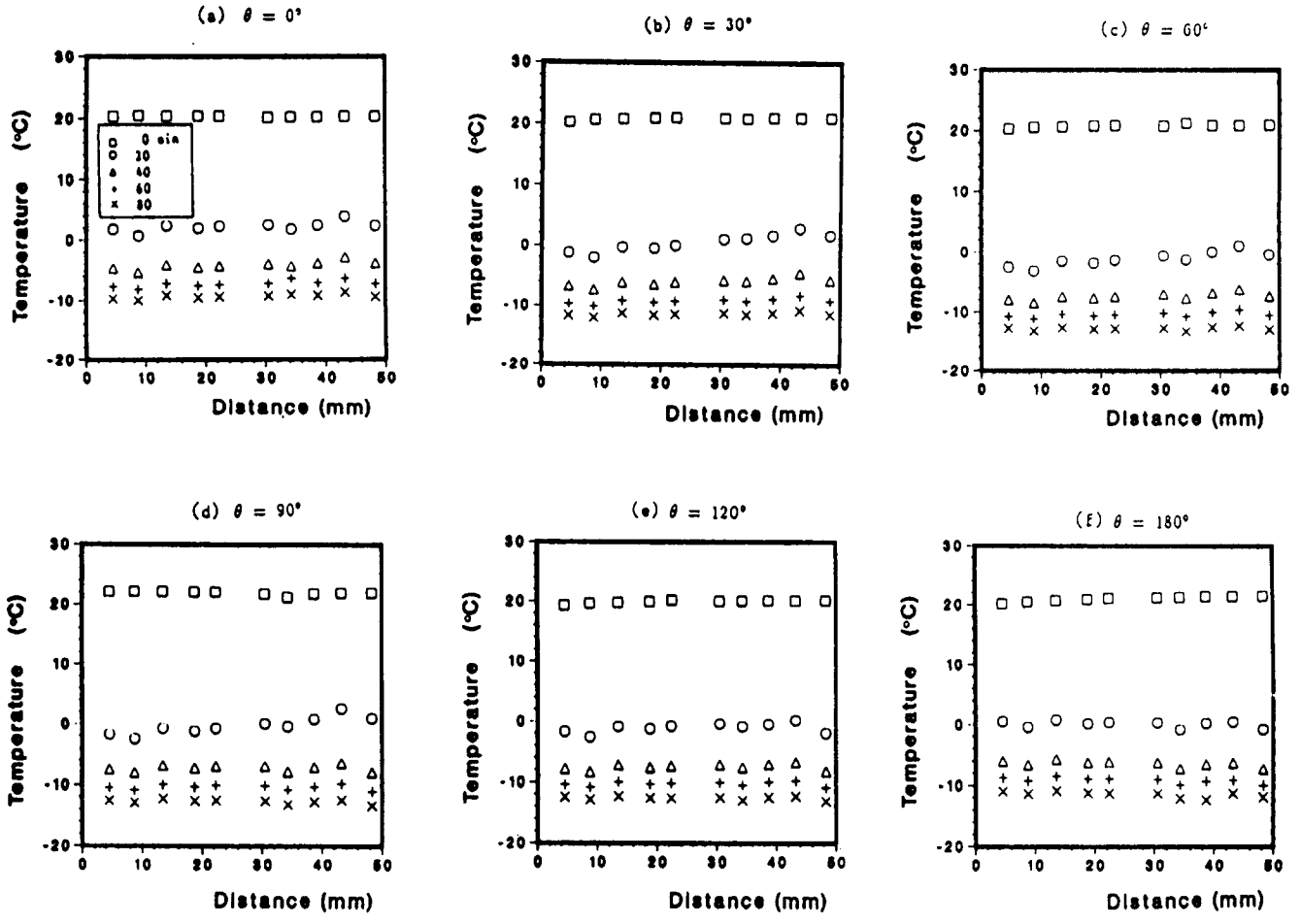

Figure 7 Temperature distribution at the centerline parallel to the cold wall in the steel-bead bed ($C_i = 5$ wt-percent). The distance is measured away from the left wall of the cavity

$C_i = 25$ wt-percent (Figure 8b), the impact of the fluid flow resulting from the double-diffusive convection is visible at all angles. This effect is more discernable at $\theta = 60°$, 90° and 120°. In these cases, the solid/mush interface is clearly 2-D. Furthermore, the frozen region grows faster towards the bottom wall of the enclosure. An additional reason for the undulated shape of this interface is the random packing of the beads, which affects the initiation of freezing in the crevices.

Figures 9a and 9b show the shapes of the solid/mush interface for the steel-bead bed for $C_i = 5$ wt-percent and $C_i = 25$ wt-percent, respectively. As expected, in the steel-bead matrix (high thermal conductivity), the freezing progressed significantly faster than the freezing in the glass-bead matrix (Figure 8). For example, for $\theta = 0°$, $C_i = 5$ wt-percent, and at $t = 75$ minutes the frozen region occupied almost 85 percent of the enclosed porous bed in the steel-bead bed, as opposed to approximately 40 percent of the enclosed space in the glass-bead bed. A similar trend in freezing rate was observed for $C_i = 25$ wt-percent. The interface shapes in Figure 9 are considerably less affected by the convective flow than the interfaces in Figure 8.

Figures 10a and 10b show the dependence of the growth of the solidified region on the inclination angle and on time for the glass-bead bed and the steel-bead bed, respectively. Each figure contains the data points for $C_i = 5$ wt-percent as well as for $C_i = 25$ wt-percent. Note that the solidified volume fraction is normalized with respect to the total volume of the cavity ($V^* = V/V_T$). The time is nondimensionalized as follows:

$$\tau = \frac{\alpha_{ms} t}{H^2} \frac{(T_i - T_{eut})C_{ms}}{L} = \text{Fo} \cdot \text{Ste} \tag{1}$$

which represents the product of the Fourier number and the Steafan number.

The volume of the frozen layer increases monotonically with time for all angles of inclination. Its dependence on the orientation angle is not as straightforward. Furthermore, for $C_i = 5$ wt-percent as well as for $C_i = 25$ wt-percent, at any given time and for any inclination angle, there is more solid formed in the steel-bead matrix than in the glass-bead matrix. Clearly, for both beds of beads the initial concentration has a profound effect on the frozen solid for all the inclination angles.

From a practical standpoint, it is desirable to have a correlation quantifying the dependence of the volume of the solidified region V^* on the inclination angle, on time, and on the initial concentration in each bed. To this end, the data points shown in Figure 10 are cast into the form of four engineering correlations utilizing regression analysis (Draper and Smith 1981). All four correlations (one for each type of bed and initial salt concentration) are summarized in the following generic form:

$$V^* = A\tau^{\beta} e^{\varepsilon \cos(\theta + \psi)} \tag{2}$$

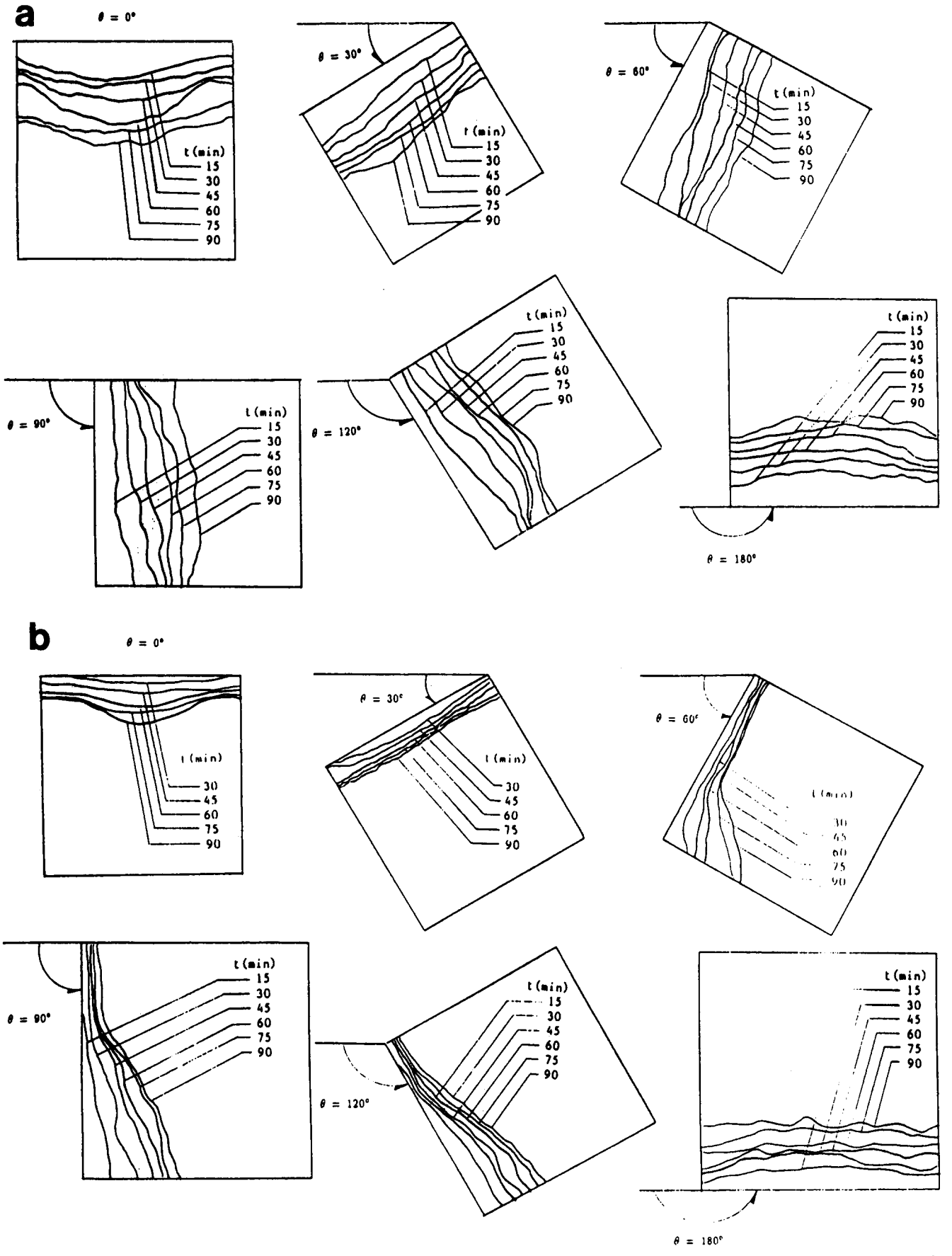

Figure 8 The growth of the solid/mush interface in the glass-bead bed for different inclination angles: (a) $C_i = 5$ wt-percent; (b) $C_i = 25$ wt-percent

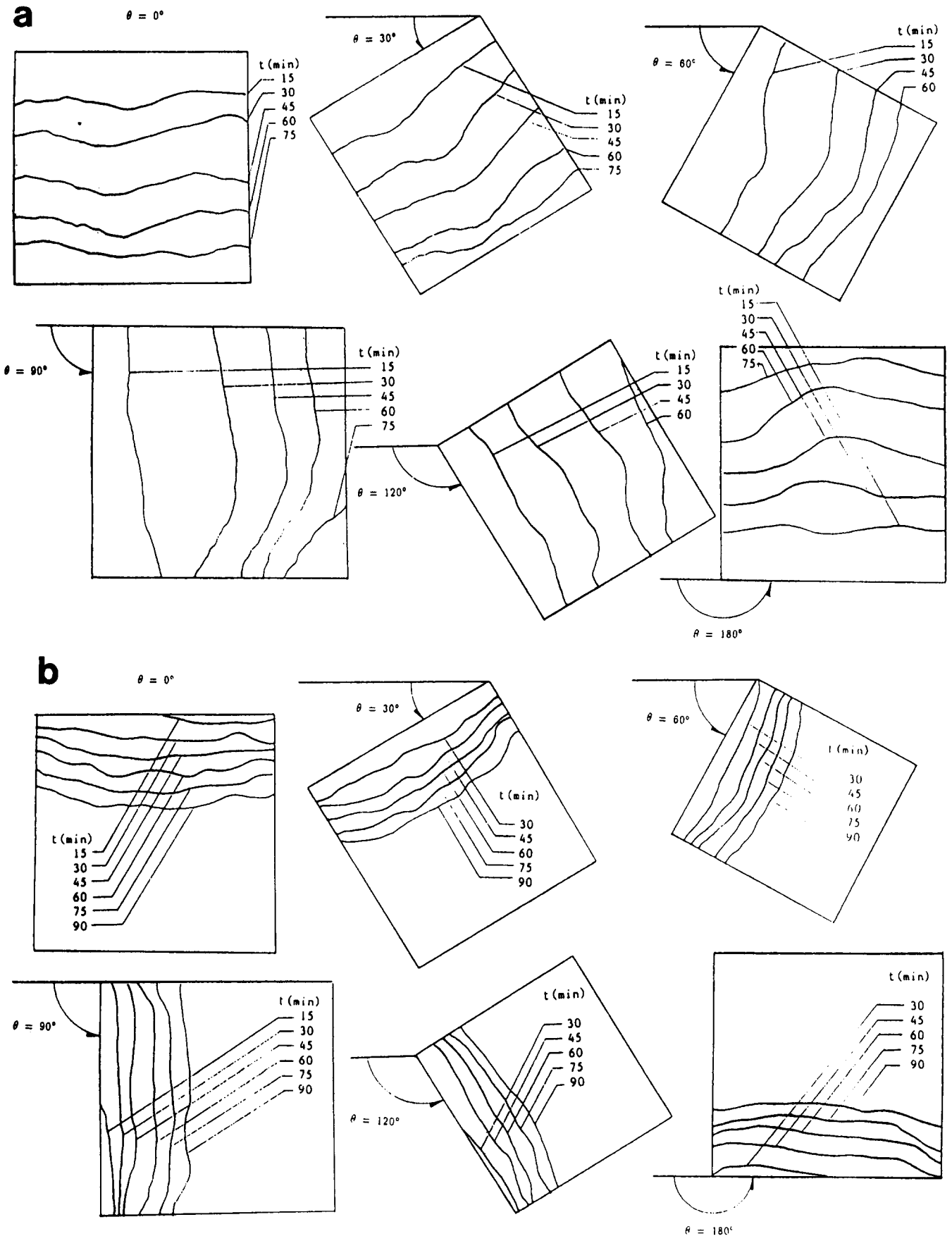

Figure 9 The growth of the solid/mush interface in the steel-bead bed for different inclination angles: (a) $C_i = 5$ wt-percent; (b) $C_i = 25$ wt-percent

Table 1 Summary of the constants appearing in the correlation (Equation 1)

Constant	Glass beads		Steel beads	
	Correlation 1 C_i = 5 wt%	Correlation 2 C_i = 25 wt%	Correlation3 C_i = 5 wt%	Correlation 4 C_i = 25 wt%
A	2.7175	1.0791	8.5040	5.3515
β	0.6889	0.8937	0.7717	1.4513
ε	−0.1037	−0.3094	0.1149	0.1300
ψ	120.59	0.33	−96.95	−26.85

where the values of various constants A, β, ε, and ψ appearing in the above correlation are tabulated in Table 1 for each specific case. The comparison of the predictions of the solid volume, produced from the correlations, with the experimental data is shown in Figure 10 (the solid lines represent the predictions from the correlations). For the purpose of engineering estimates, the correlations perform well for all cases.

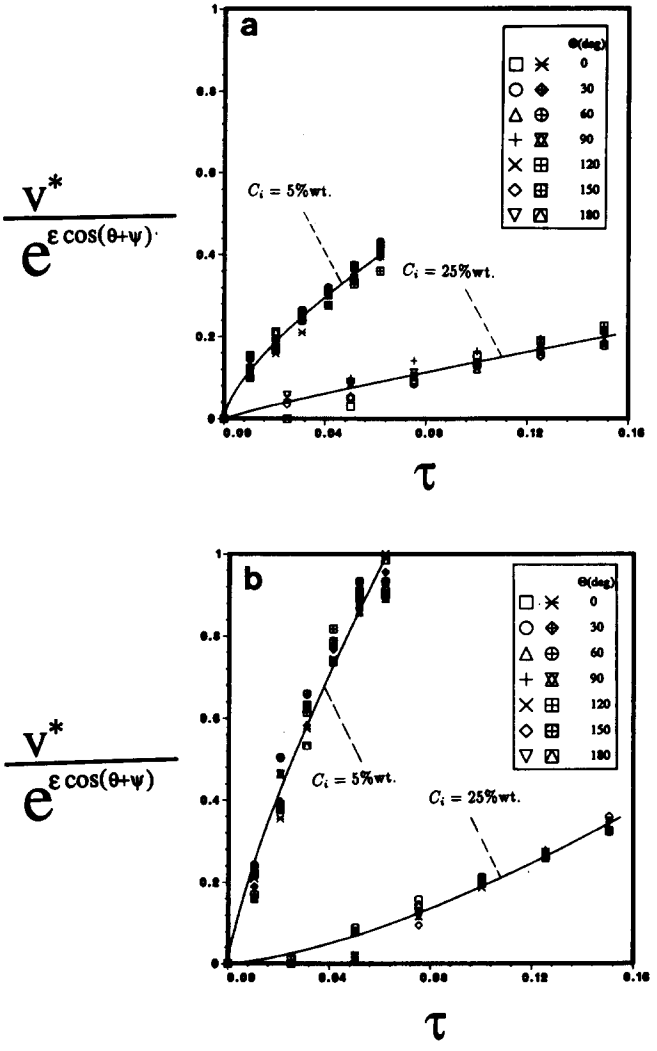

Figure 10 A comparison between the correlations (Equation 1 and Table 1) and the experimental data for the volume of the solidified region: (a) glass beads; (b) steel beads

Conclusions

An experimental study of solidification of a porous matrix saturated with a binary mixture (H_2O–NH_4Cl) enclosed in an inclined rectangular cavity with one cold wall and five adiabatic walls was conducted. The results obtained for two types of porous beds, namely, a glass-bead bed and a steel-bead bed, were reported. Two representative initial salt concentrations were examined on either side of the eutectic point in the phase equilibrium diagram of the H_2O–NH_4Cl system (5 wt-percent and 25 wt-percent).

The temperature field characterized by the temperature distribution along the centerline perpendicular and parallel to the cold wall affirmed the presence of the convective flow in the system as a result of the thermal and the compositional gradients. This flow was stronger in the glass-bead system compared to the steel-bead system where conduction was dominant at all times and for all angles. Furthermore, it was observed that convection was more vivid for the initial concentration of 5 wt-percent (below eutectic). The inclination angle of the cold wall had a significant effect on the convective flow and therefore on the solidification process.

The evolution of the freezing process was observed from the solid/mush interface position. The shape of this interface verified the fact that conduction was the dominant heat transfer mode in the steel-bead bed.

To quantify the dependence of the volume of the frozen region on the inclination angle, on time, and on the initial concentration, four engineering correlations (Equation 2 and Table 1) were obtained and were reported in this paper.

References

Benenati, R. F. and Brosilow, C. B. 1962. Void fraction distribution in packed beds. *AICHE J.*, **8**, 359–361

Bennon, W. D. and Incropera, F. P. 1987a. A continuum model for momentum, heat and species transport in binary solid-liquid phase change systems-I. Model formulation. *Int. J. Heat Mass Transfer*, **30**, 2161–2170

Bennon, W. D. and Incropera, F. P. 1987b. A continuum model for momentum, heat and species transport in binary solid-liquid phase change systems-II. Application to solidification in a rectangular cavity. *Int. J. Heat Mass Transfer*, **30**, 2171–2187

Cao, W.-Z. and Poulikakos, D. 1990. Solidification of an alloy in a cavity cooled through its top surface. *Int. J. Heat Mass Transfer*, **33**, 427–434

Cao, W.-Z. and Poulikakos, D. 1991. Freezing of a binary alloy saturating a packed bed of spheres. *AIAA J. Thermophys.*, **5**(1), 46–53

Chandrasekhara, B. C. and Vortmeyer, D. 1979. Flow model for velocity distribution in fixed beds under isothermal conditions. *Warme and Stoffubertragung*, **12**, 105–111

Chellaiah, S. and Viskanta, R. 1987. Freezing of salt solutions on a vertical wall. *Exp. Heat Transfer*, **1**, 181–195

Chellaiah, S. and Viskanta, R. 1988. Freezing of saturated and

superheated liquid in porous media. *Int. J. Heat Mass Transfer*, **31**, 321–330

Chellaiah, S. and Viskanta, R. 1989. Freezing of water-saturated porous media in the presence of natural convection: Experiments and analysis. *J. Heat Transfer*, **111**, 425–432

Chen, C. F. and Chen, F. 1991. Experimental study of directional solidification of aqueous ammonium chloride solution. *J. Fluid Mech.*, **427**, 567–586

Christenson, M. S. and Incropera, F. P. 1989. Solidification of an aqueous ammonium chloride solution in a rectangular cavity-I. Experimental Study. *Int. J. Heat Mass Transfer*, **32**, 47–68

Draper, N. R. and Smith, H. 1981. *Applied Regression Analysis.* John Wiley & Sons, New York

Frivik, P. E. and Comini, G. 1982. Seepage of heat flow in soil freezing. *J. Heat Transfer*, **104**, 323–328

Goldstein, M. E. and Reid, R. L. 1978. Effect of fluid flow on freezing and thawing of saturated porous media. *Proc. R. Soc. Lond. Ser. A*, **364**, 45–73

Gupta, J. P. and Churchill, S. W. 1971. Heat and moisture transfer in sand during freezing. *Proc. Winter Annual Meeting of ASME*, **HTD-4**, Vol. 4, ASME, Washington, DC, 99–105

Hashemi, H. T. and Slipcevich, C. M. 1973. Effect of seepage stream on artificial soil freezing. *ASCEJ Mech. Foundation Design*, **99**, 267–289

Huppert, H. E. 1990. The fluid mechanics of solidification. *J. Fluid Mech.*, **212**, 209–240

Kececioglu, I. and Rubinsky, B. 1989. A continuum model for the propagation of discrete phase-change fronts in porous media in the presence of coupled heat flow, fluid flow and species transport processes. *Int. J. Heat Mass Transfer*, **32**, 1111–1130

Stephen, H. and Stephen, T. (eds.). 1963. *Solubilities of Inorganic and Organic Compounds*, Vol. 1. Pergamon Press, New York, 212–213

Sugawara, M., Imaba, H., and Seki, N. 1988. Effect on maximum density of water on freezing of a water-saturated horizontal porous layer. *J. Heat Transfer*, **110**, 155–159

Thompson, M. E. and Szekely, J. 1988. Mathematical and physical modeling of double-diffusive convection of aqueous solutions crystallizing at a vertical well. *J. Fluid Mech.*, **187**, 409–433

Weaver, J. A. and Viskanta, R. 1986. Freezing of liquid-saturated porous media. *J. Heat Transfer*, **108**, 654–659

Yang, C.-H. 1992. *Solidification of a Pure Liquid and a Binary Mixture in an Inclined Rectangular Bed of Spheres.* M.S. thesis, Mechanical Engineering Dept., The University of Illinois at Chicago, Chicago, IL